Chemical Senses, 2017, Vol 42, 759–767
doi:10.1093/chemse/bjx055
Original Article
Advance Access publication August 18, 2017

Original Article

Type III Cells in Anterior Taste Fields Are More Immunohistochemically Diverse Than Those of Posterior Taste Fields in Mice

Courtney E. Wilson[1,2,3], Thomas E. Finger[1,3,4] and Sue C. Kinnamon[1,2,3]

[1]Rocky Mountain Taste and Smell Center, University of Colorado School of Medicine, Aurora, CO 80045, USA, [2]Department of Otolaryngology, University of Colorado School of Medicine, Aurora, CO 80045, USA, [3]Neuroscience Graduate Program, University of Colorado School of Medicine, Aurora, CO 80045, USA, [4]Department of Cell and Developmental Biology, University of Colorado School of Medicine, Aurora, CO 80045, USA

Correspondence should be sent to: Courtney E. Wilson, Department of Otolaryngology, University of Colorado School of Medicine, 12700 E. 19th Ave, Mail Stop 8606, Aurora, CO 80045, USA. e-mail: courtney.wilson@ucdenver.edu

Editorial Decision 11 August 2017.

Abstract

Activation of Type III cells in mammalian taste buds is implicated in the transduction of acids (sour) and salty stimuli. Several lines of evidence suggest that function of Type III cells in the anterior taste fields may differ from that of Type III cells in posterior taste fields. Underlying anatomy to support this observation is, however, scant. Most existing immunohistochemical data characterizing this cell type focus on circumvallate taste buds in the posterior tongue. Equivalent data from anterior taste fields—fungiform papillae and soft palate—are lacking. Here, we compare Type III cells in four taste fields: fungiform, soft palate, circumvallate, and foliate in terms of reactivity to four canonical markers of Type III cells: polycystic kidney disease 2-like 1 (PKD2L1), synaptosomal associated protein 25 (SNAP25), serotonin (5-HT), and glutamate decarboxylase 67 (GAD67). Our findings indicate that while PKD2L1, 5-HT, and SNAP25 are highly coincident in posterior taste fields, they diverge in anterior taste fields. In particular, a subset of taste cells expresses PKD2L1 without the synaptic markers, and a subset of SNAP25 cells lacks expression of PKD2L1. In posterior taste fields, GAD67-positive cells are a subset of PKD2L1 expressing taste cells, but anterior taste fields also contain a significant population of GAD67-only expressing cells. These differences in expression patterns may underlie the observed functional differences between anterior and posterior taste fields.

Key words: fungiform, GABA, PKD2L1, salty, serotonin, sour

Introduction

Type III cells of taste buds are the only cell type that forms classical chemical synapses onto gustatory nerve fibers complete with neurotransmitter-containing synaptic vesicles (Murray and Murray 1971; Royer and Kinnamon 1991). In contrast, Type II cells form unusual synapses that rely on atypical mitochondria and large-pore ATP release channels (Royer and Kinnamon 1988; Taruno et al. 2013). Type I cells are generally considered to be glial-like support cells (Murray 1993; Pumplin et al. 1997). In addition to their structural differences, Type III cells are functionally different from the other cell types: Type III cells transduce acids (sour) and various electrolytes and express ion channels that are sensitive to acids (Huang et al. 2006; Chang et al. 2010; Oka et al. 2013; Ye et al. 2016), whereas Type II cells mediate detection of umami, sweet, and bitter stimuli by means of G-protein-coupled receptors and a phospholipase C (PLC)-mediated transduction cascade (Clapp et al. 2004; DeFazio et al. 2006). Although the

diversity of molecular and functional characteristics of Type II cells is well established, the situation in regard to Type III cells is less clear.

The original defining characteristics of Type III cells were ultrastructural—they feature synaptic vesicles and a conventional morphology of chemical synapses. Subsequent study revealed that cells with this characteristic shared other properties, including accumulation and release of three classical neurotransmitters: 5-HT (Nada and Hirata 1975; Fujimoto et al. 1987; Kim and Roper 1995; Yee et al. 2001; Huang et al. 2005), GABA (Dvoryanchikov et al. 2007, Dvoryanchikov et al. 2011; Huang et al. 2011), and norepinephrine (Dvoryanchikov et al. 2007; Huang et al. 2008). These cells were also soon associated with the expression of SNAP25 (a marker of synaptic vesicles) (Yang et al. 2000; Clapp et al. 2004), voltage-gated calcium channels, and increased capacitance consistent with release of vesicles upon activation (Roberts et al. 2009; Vandenbeuch et al. 2010). Because of the presence of voltage-gated calcium channels, isolated Type III taste cells exhibit calcium influx in response to extracellular application of KCl—this has been a defining characteristic in many physiological studies (Huang et al. 2007; Huang et al. 2011). Yet, physiological differences in Type III cell function have been noted between anterior taste fields innervated by branches of the 7th cranial nerve (fungiform papillae and palate) and posterior taste fields innervated by the 9th cranial nerve (foliate and circumvallate papillae). In posterior taste fields, for example, the large majority of Type III cells respond to both acids and salts (Tomchik et al. 2007), whereas in taste buds from fungiform papillae, most Type III cells respond only to acids while a smaller subset respond to both acids and NaCl (Yoshida et al. 2009). In addition to responding directly to acids and salts, some Type III cells also respond indirectly to stimuli transduced by Type II cells, via ATP released by Type II cells during transduction (for review, Roper 2013; Chaudhari 2014). These "broadly tuned" Type III cells are considerably more abundant in posterior tongue than anterior tongue (Yoshida et al. 2009).

Because of the evidence for diversity in Type III cell function, we tested whether there was a similar diversity in molecular features of Type III cells in anterior and posterior taste fields. We utilized the marker PKD2L1 as our foundational indicator for Type III cell identity because this molecule is associated with sour taste function (Huang et al. 2006; Chang et al. 2010) and has been localized to cells identified by electron microscopy as containing classical synapses (Kataoka et al. 2008). We compared anterior and posterior taste fields for differences in the expression pattern of PKD2L1 with other features associated with Type III cells: 5-HT, SNAP25, and GAD67 (for GABA).

Materials and methods

Mice

All mice were housed at the University of Colorado Anschutz Medical Campus on a 12 h/12 h light/dark cycle and had constant access to standard chow. All procedures were approved by the Animal Care and Use Committee at the University of Colorado School of Medicine. To avoid the complications of using separate rabbit-derived antibodies on the same tissue, we used a BAC transgenic PKD2L1-YFP mouse (donated by Dr Emily Liman) to visualize PKD2L1-expressing cells in most experiments (Chang et al. 2010). In this mouse, yellow fluorescent protein is expressed under the *Pkd2l1* promoter. Fidelity of YFP expression in this mouse was verified in the present paper, using a validated antibody against PKD2L1. In the experiments visualizing GAD67, we used a GAD67-GFP transgenic mouse (Jax stock #007677), which expresses green fluorescent protein under the *Gad67* promoter (Chattopadhyaya et al. 2004; Tomchik et al. 2007). For each investigated marker (5-HT, SNAP25, GAD67), tissue from 4 mice contributed to the final data sets.

Perfusion/fixation

To fix and obtain taste tissues, mice were anesthetized with sodium pentobarbital, i.p. injection at 50 mg/kg, and transcardially perfused with 4% paraformaldehyde (PFA; SIGMA cat#158127). Tongues and soft palate tissues were extracted before immersion in 4% PFA for 1.5–6 h. In one mouse used for 5-HT imaging, 4% periodate-lysine-PFA fixative (L-lysine monohydrochloride SIGMA cat#L-5626; sodium periodate SIGMA cat#S-1147; 1.6% PFA) was used in place of PFA—results between the two fixation techniques did not differ. To label serotonin-accumulating cells, PKD2L1-YFP transgenic mice were injected with 5-hydroxy-l-tryptophan (SIGMA cat#H-9772) at a concentration of 80 mg/kg 1 h prior to anesthetic injection. After fixation and post-fix PFA treatment, tissues were transferred to a 20% sucrose solution overnight at 4 °C before being mounted in optimal cutting temperature (OCT) compound (Fisher Healthcare) and cut into 12–16 µm slices via cryostat. Tissue was then collected onto slides (Tanner Scientific) in a 1:10 series and stored at −20 °C.

Immunohistochemistry

Before antibody staining, slides were washed in 0.1 M phosphate-buffered saline (PBS; monobasic sodium phosphate SIGMA cat#S-5011; dibasic sodium phosphate SIGMA cat#S-0876; sodium chloride SIGMA cat#S-7653) 3 times for 10 min each on a shaker. A blocking solution of 2% Normal Donkey Serum in blocking buffer (0.1M PBS + 0.3% triton x-100 USB cat#22686, 1% bovine serum albumin SIGMA cat#A-7906) was applied in darkness, at room temperature, for an hour. Slides were then incubated with one or more of the following primary antibodies in darkness, at 4 °C, overnight (Table 1). Control slides were incubated with blocking buffer without primary antibody. Before the secondary antibody was applied, slides were washed in 0.1 M PBS 3 times for 10 min each. Secondary antibodies were applied to each slide for 3 h, in darkness, at room temperature (Table 2). For GAD67-GFP experiments,

Table 1. List of primary antisera

Target protein	Host	Dilution	Manufacturer	Cat number	RRID	Lot
GFP	Chicken	1:2000	Aves	GFP-1020	AB_10000240	0511FP12
PKD2L1	Rabbit	1:500	Hiroaki Matsunami Lab, Duke University Medical Center	PKD2L1	AB_2661860	N/A
SNAP25	Goat	1:1000	GeneTex	GTX89577	AB_10724125	821604337
P2X3	Rabbit	1:200	Alomone	APR-016	AB_2040056	APR016AN0802
5-HT	Rabbit	1:2500	Immunostar	20080	AB_572263	1431001
PLCβ2	Rabbit	1:200	Santa Cruz	Sc-206	AB_632197	A1204

DRAQ5 (abcam #ab108410) was added to the secondary antibody incubation solutions at a concentration of 1:5000 to visualize cell nuclei in far red. DAPI staining allowed for the identification of taste buds in the epifluorescent microscope but could not be imaged in the absence of an appropriate laser. DRAQ5, therefore, allowed for the imaging of nuclear stain. After the secondary incubation, slides were washed in 1:10,000 DAPI (Life technologies REF#03571) in 0.1 M PBS. Slides were subsequently washed in 0.1M PBS for 10 min and 0.05 M PBS before applying coverslips (Southern Biotech Fluoromount-G cat#0100-01; VWR cat#48393 251).

Imaging and cell counting

All tissues were imaged on a Leica S5 confocal microscope, with Leica LAS AF software version 2.7.3.9723. Taste buds were identified visually via DAPI fluorescence and subsequently imaged with a 40× oil immersion N.A. 1.25 lens. Cells were counted in the following manner: First, each channel in an image was converted to a binary image with a modified Otsu method in ImageJ (1.49 v, NIH public domain). The channels were then combined to form a composite image. Cells were counted with the ImageJ plug-in cell counter. Profiles were considered to be cells of interest if, in either marker channel, the image showed both: (i) a clear nucleus and (ii) an elongate apical process. If the profile of interest contained positive fluorescence in any part of the profile, it was considered positive for that particular marker. As markers are sometimes expressed in separate subcellular locations, this technique provided greater accuracy than strict pixel colocalization analysis. For GAD67-GFP experiments, DRAQ5 fluorescence allowed for cell identification via nuclear staining. In SNAP25 experiments, rabbit anti-P2X3 staining took the place of DRAQ5 in the far red region, so counts were performed in the absence of nuclear staining. In 5-HT experiments, optical bleed-through necessitated that 5-HT be visualized in far red, so counts were performed in same manner. Venn Diagram Plotter (Kyle Littlefield, DOE, 2004) was used to create the to-scale Venn

Table 2. List of secondary antisera

Target species	Host	Dilution	Manufacturer	Cat number	RRID	Wavelength
Chicken	Donkey	1:400	Jackson Immunoresearch	703-545-155	AB_2340375	488
Rabbit	Donkey	1:400	Molecular Probes	A10042	AB_11180183	568
Goat	Donkey	1:400	Molecular Probes	A21447	AB_141844	647

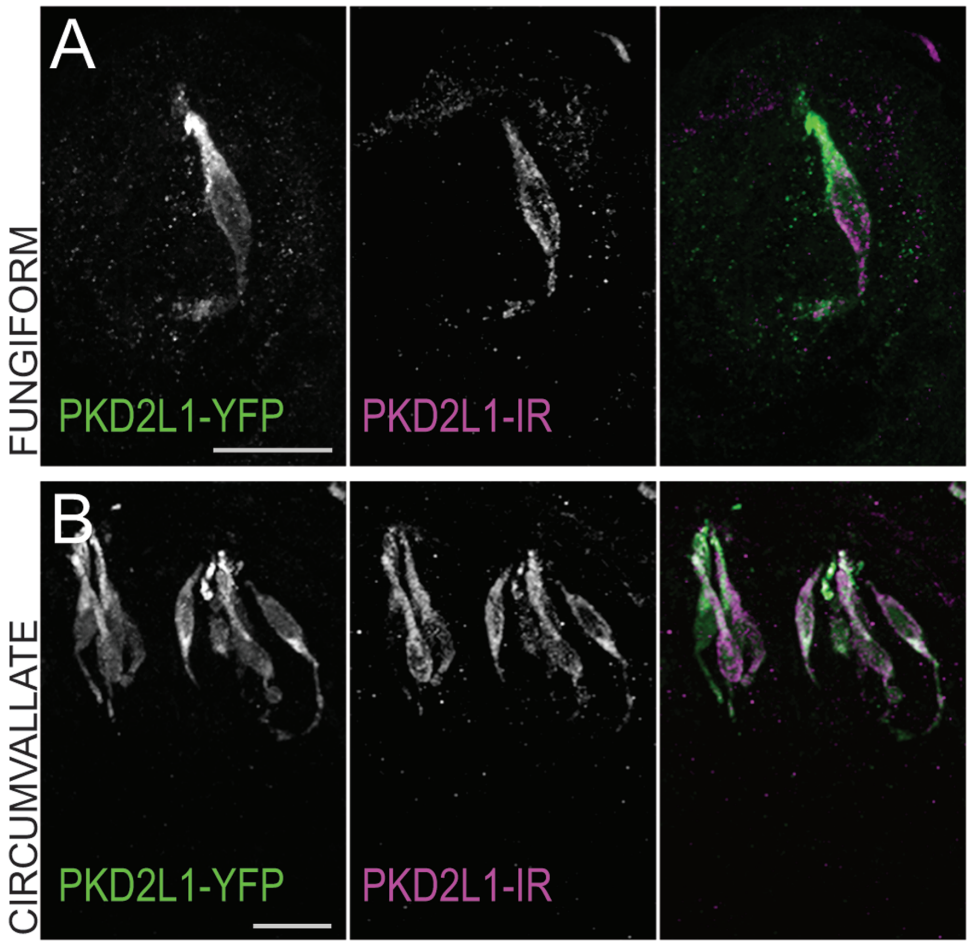

Figure 1. Transgenic PKD2L1-YFP mice display immunofluorescence in PKD2L1 immunoreactive cells. Confocal z-stack images of (**A**) fungiform and (**B**) circumvallate taste buds from a PKD2L1-YFP transgenic mouse showing PKD2L1-YFP fluorescence in green and PKD2L1 immunoreactivity in magenta. Scale bars = 20 μm. In all tissues, the 2 markers are coincident.

diagrams, and Adobe Photoshop and Indesign were used to formulate photos and figures. Statistics were performed with Prism 7 (GraphPad software Inc., La Jolla, CA).

Results

Polycystic kidney disease 2-like 1 (PKD2L1) served as the central marker of our immunohistochemical experiments. We used a transgenic PKD2L1-YFP mouse to visualize PKD2L1 expression in most experiments. PKD2L1-YFP-positive fluorescent cell profiles were spindle shaped, most often with extensions toward the pore of the taste bud and cell diameters that ranged from ~2.2 to 7.7 µm. Out of 15 sample cells from each population, cell profile width did not differ between fungiform (4.55 ± 1.21 µm) and circumvallate (4.95 ± 0.94 µm) PKD2L1-YFP cell profiles (unpaired *t*-test, $P = 0.291$). Taste buds in the nasoincisor papilla were similar to fungiform papillae in that they tended to contain few PKD2L1-positive cells. Our sample size for nasoincisor taste buds was too small to make definitive conclusions. In one mouse, we confirmed that YFP fluorescence in this line is coincident with a previously validated PKD2L1 antibody (Ishimaru et al. 2006) in all fungiform, soft palate, circumvallate, and foliate taste buds (Figure 1). These data corroborate previous results using this mouse (Chang et al. 2010).

5-HT

Though largely coincident, the 5-HT and PKD2L1-YFP populations diverge slightly in anterior taste fields (~79% coincidence) as compared to posterior taste fields (~92% coincidence) (Figure 2). Neither anterior (fungiform and soft palate) nor posterior taste field papillae (circumvallate and foliate) were significantly different within fields according to separate chi-square tests ($P = 0.6833$ and $P = 0.3094$, respectively). Pooled anterior field counts were, however, significantly different from pooled posterior field counts ($P = 0.0002$), with a greater proportion of single-labeled cells, both 5-HT only and PKD2L1 only, in the anterior than in the posterior fields. Total

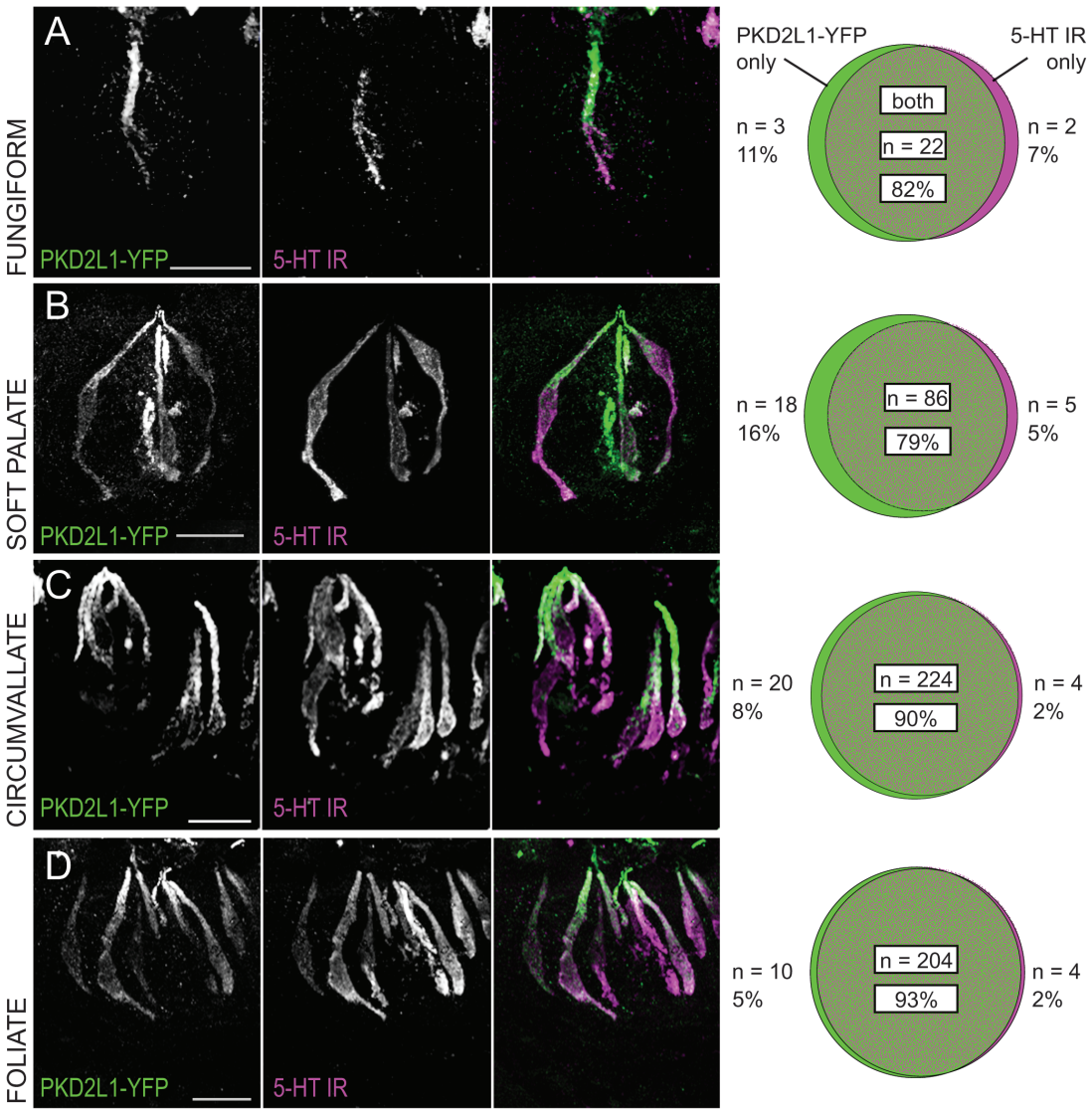

Figure 2. Coincidence between 5-HT immunoreactivity and PKD2L1-YFP fluorescence is higher in posterior than in anterior taste fields. (Left) Confocal z-stack images of (**A**) fungiform, (**B**) soft palate, (**C**) circumvallate, and (**D**) foliate taste buds in transgenic PKD2L1-YFP mice injected with 5-HTP, the 5-HT precursor. PKD2L1-YFP fluorescence is shown in green, and 5-HT immunoreactivity is shown in magenta. All scale bars = 20 µm. (Right) Venn diagrams show coincidence of fluorescent markers in each taste field. Anterior and posterior cell distributions were different according to a chi-square test, $P = 0.0002$.

cells counted in anterior taste fields are lower than those of posterior taste fields in this and following comparisons, owing to the relative scarcity of Type III taste cells in anterior taste buds (Ma et al. 2007; Ohtubo and Yoshii 2011).

SNAP25

The expression of SNAP25 in nerve fibers as well as in Type III taste cells tends to confound our ability to delineate taste receptor cells clearly from innervating fibers. To circumvent this confound, we costained the tissue with antibody against the purinergic receptor P2X3, which is expressed in nerve fibers, but not in taste cells (Bo et al. 1999). Thus, double-labeled profiles were assumed to be nerve fibers and excluded from counting.

Both SNAP25 and PKD2L1-YFP appear largely coincident (~94%) in taste cells of circumvallate and foliate taste buds. Although substantial overlap of markers (~73%) does occur in the anterior taste fields (fungiform and soft palate taste buds), the proportion of colocalized cells is lower (Figure 3). Chi-square tests indicate that the

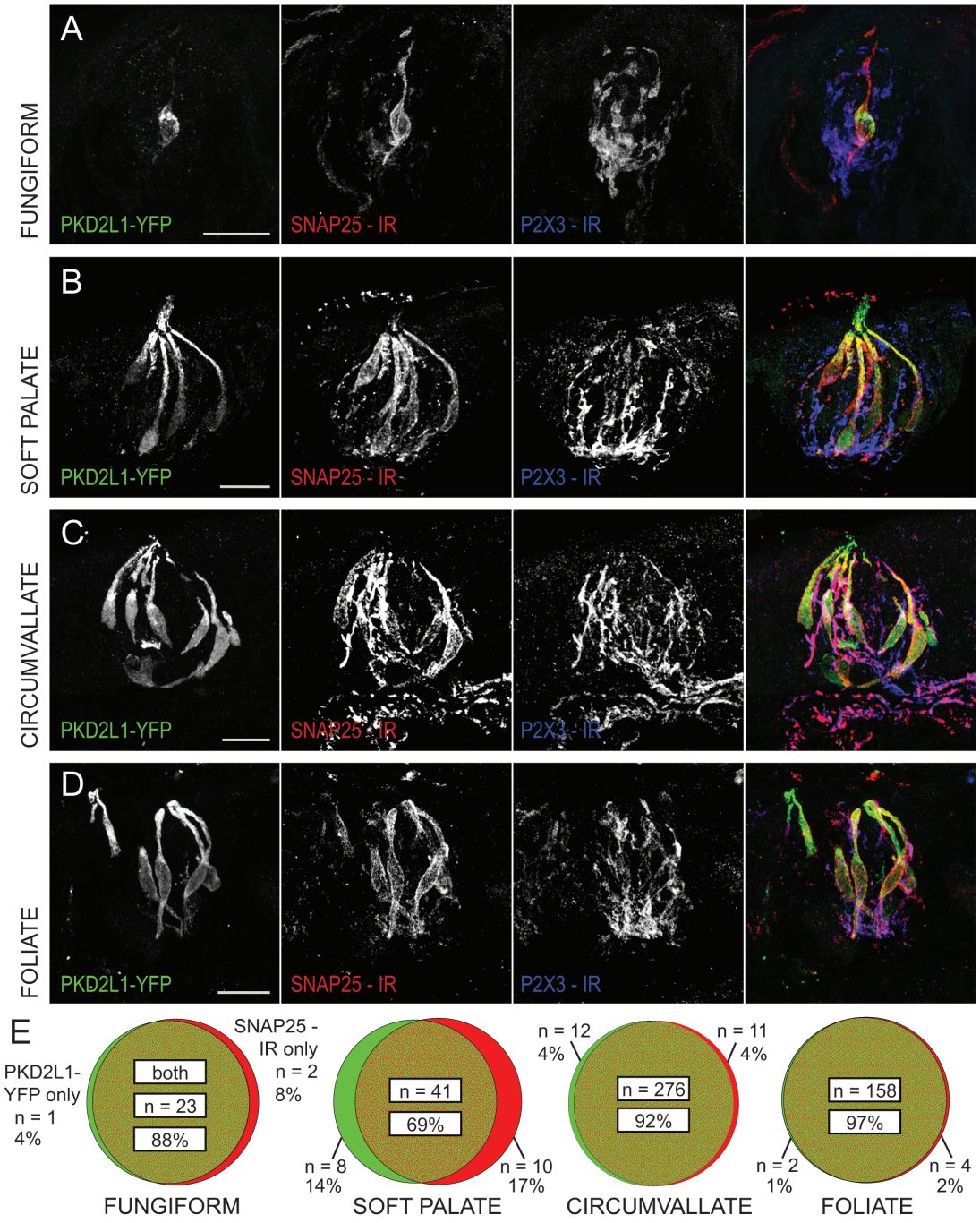

Figure 3. Coincidence between SNAP25 immunoreactivity and PKD2L1-YFP fluorescence is greater in posterior taste fields than in anterior taste fields. Confocal z-stack images of (**A**) fungiform, (**B**) soft palate, (**C**) circumvallate, and (**D**) foliate taste buds in transgenic PKD2L1-YFP mice. PKD2L1-YFP fluorescence is shown in green, SNAP25 immunoreactivity is shown in red, and P2X3 immunoreactivity is shown in blue to exclude SNAP25-positive nerve fibers from the cell count. All scale bars = 20 μm. (**E**) Venn diagrams show high coincidence of fluorescent PKD2L1 and SNAP25 marker in posterior taste fields and a lower coincidence in anterior taste fields. Chi-square test revealed a significant difference between the distributions of anterior and posterior taste fields, $P < 0.0001$.

cell count distribution in the fungiform taste field is *not* significantly different from that of the soft palate ($P = 0.0942$) and that the distribution in the circumvallate field is *not* different from that of the foliate ($P = 0.1808$). We thus combined these groups for further analysis. A chi-square test comparing anterior to posterior data revealed a significant difference in cell distribution between the two taste fields ($P < 0.0001$), with anterior taste field featuring an increased proportion of single-labeled cells, both SNAP25 only and PKD2L1 only.

GAD67

To test for coexpression of GAD67 and PKD2L1, we used a transgenic GAD67-GFP mouse (Chattopadhyaya et al. 2004) that has been used as a reporter in numerous studies of Type III cell function (Tomchik et al. 2007; Yoshida et al. 2009; Vandenbeuch et al. 2010; Dvoryanchikov et al. 2011). GFP expression in this mouse is known to be restricted to Type III cells in circumvallate taste buds (Tomchik et al. 2007), but its selective expression has not been adequately validated in other taste fields. We examined GFP expression against the Type II cell marker phospholipase C beta 2 (PLCβ2) using immunohistochemistry. No overlap of expression was present in any taste field (Figure 4), validating the use of the mouse for further experiments.

The data comparing GAD67-GFP fluorescence to PKD2L1 immunoreactivity reveals that, in the circumvallate and foliate fields, GFP fluorescence appears in a subset of PKD2L1 immunoreactive cells. These data align with previous characterizations of GAD67-GFP expression (Tomchik et al. 2007). In the anterior fields, however, the expression profile was surprisingly different. In fungiform and soft palate tissue, a sizable cohort of GAD67-GFP-positive cells (~18%) does not display PKD2L1 immunoreactivity (Figure 5). By extension, these data suggest that anterior fields host a population of GAD67-positive cells that *do not* express SNAP25. This conclusion is supported by subsequent data from one mouse indicating a population of GAD67-GFP-positive cells that do not react with the anti-SNAP25 antibody (Figure 6). Cell counts between GAD67-GFP and PKD2L1-IR cells in the fungiform and soft palate fields were not different from each other according to a chi-square test ($P = 0.4401$). We therefore pooled the anterior data and compared it to both circumvallate and foliate cell counts with chi-square tests. In both cases, the differences between groups were statistically significant ($P < 0.0001$ for both). In anterior taste fields, single-labeled cells of both markers exist, whereas in posterior taste fields, GAD67-GFP-positive cells are a subset of PKD2L1-IR cells.

Discussion

In the present study, we show that Type III cells of the anterior and posterior taste fields differ somewhat in their phenotypic

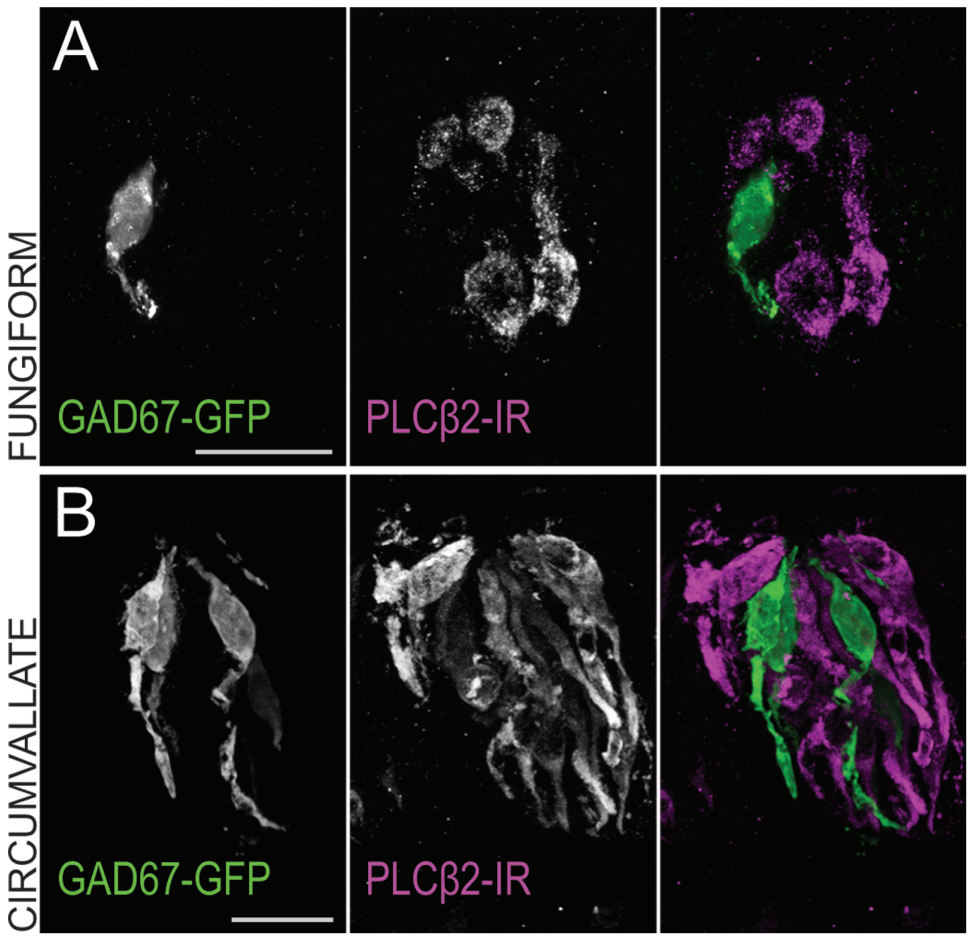

Figure 4. Transgenic GAD67-GFP mice display immunofluorescence consistent with a Type III cell population. Confocal z-stack images of (**A**) fungiform and (**B**) circumvallate taste buds from a GAD67-GFP transgenic mouse showing GAD67-GFP fluorescence in green and PLCβ2 immunoreactivity in magenta. Scale bars = 20 μm. GAD67-GFP-positive taste cells do not coincide with the Type II cell marker PLCβ2 in any taste field, nor do they share morphology with Type I cells.

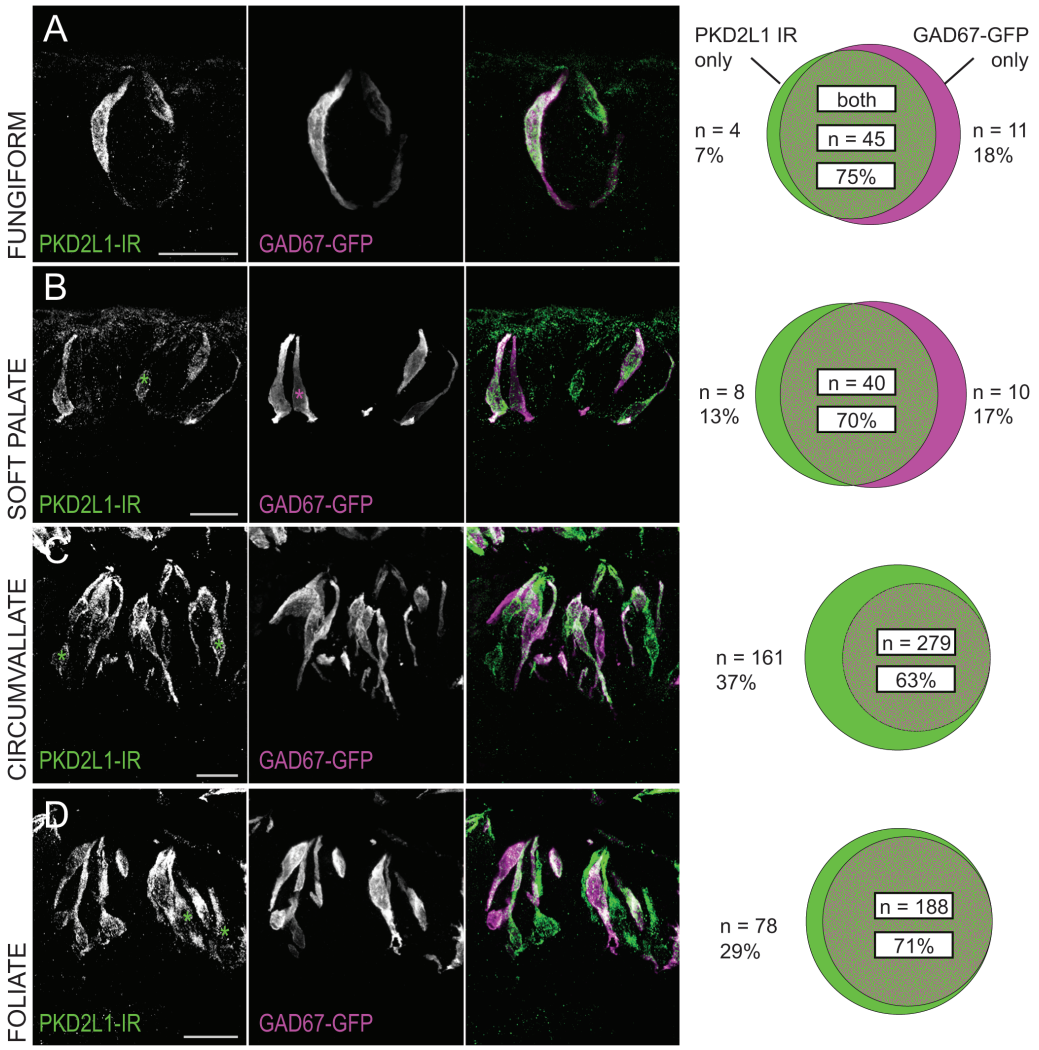

Figure 5. Coincidence between GAD67-GFP fluorescence and PKD2L1 immunoreactivity differs between posterior and anterior taste fields. (Left) Confocal z-stack images of (**A**) fungiform, (**B**) soft palate, (**C**) circumvallate, and (**D**) foliate taste buds in transgenic GAD67-GFP mice. For consistency, PKD2L1 immunoreactivity is shown in green, with asterisks marking PKD2L1-IR-only cells. GAD67-GFP fluorescence is shown in magenta, with asterisks marking GAD67-GFP-only cells. Scale bars = 20 μm. (Right) Venn diagrams show differing coincidence of GAD67-GFP and PKD2L1 immunoreactivity between posterior and anterior taste fields. The distribution of anterior taste fields is significantly different from both circumvallate and foliate distributions via a chi-square test, $P < 0.0001$ for both.

characteristics. In circumvallate and foliate fields, PKD2L1 expression largely coincides with that of 5-HT and SNAP25, whereas in fungiform and soft palate taste buds, Type III cells are more heterogeneous. While GAD67 marks a subset of the PKD2L1-positive cell population in posterior tongue, there are single-labeled cells of both markers in anterior tongue. Furthermore, both anterior taste fields contain a population of Type III taste cells that express canonical phenotypic Type III taste cell markers such as SNAP25 but do not express PKD2L1. These data serve as a caution against treating any particular Type III cell indicator as absolutely indicative of all Type III-associated functions, particularly in fungiform taste buds.

Our data largely confirm previous studies showing that PKD2L1 expression in posterior taste fields is coincident with synaptic markers (Kataoka et al. 2009) and that GAD67 expression occurs in a subset of these cells (Tomchik et al. 2007). One interesting discrepancy between our data and those of another study is that we observe some GAD67 expressing taste cells in fungiform papillae that do not express PKD2L1, although a physiological study using GAD67-GFP taste cells found that all GFP-labeled cells responded to sour taste stimuli (Yoshida et al. 2009). If PKD2L1 cells are required for transmission of sour taste information to chorda tympani nerve fibers, as indicated in Huang et al. (2006), what mechanism are the GAD67-positive, PKD2L1-negative cells using to transduce sour taste?

Some discrepancies of expression patterns in Type III cells may be the consequence of developmental changes. Our counting criteria did not distinguish between developing, mature, or senescent Type III cells. As taste cells are constantly renewing, 60–70% of the taste cells are estimated to be functional, whereas the remainder may be either dying or immature (Barlow, 2015). We collected only snapshots of a dynamic process, and our chosen markers may have differing time courses of expression across the lifetime of a cell. This caveat, however, is probably less important in Type III cells, which are longer lived than Type I or Type II cells and are thus less likely to be captured in a state of atrophy or immaturity (Perea-Martinez et al. 2013). Developmental mechanisms that regulate cell turnover and maturation may also be different between anterior and posterior taste fields. Taste progenitor cells that supply circumvallate taste buds express different markers and undergo subtly different signaling

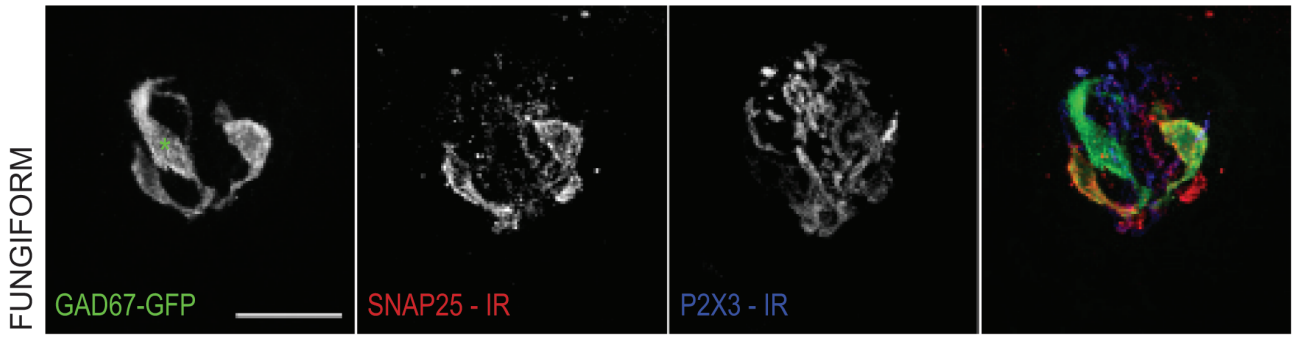

Figure 6. Example of a GAD67-GFP-positive, fungiform taste cell that is not positive for SNAP25 immunoreactivity. Confocal z-stack images of a fungiform taste bud from a transgenic GAD67-GFP mouse. GAD67-GFP fluorescence is shown in green, with an asterisk marking a GAD67-GFP-only cell. SNAP25 immunoreactivity is shown in red. P2X3 immunoreactivity is shown in blue. Scale bars = 20 µm.

mechanisms than those of the fungiform papillae (for review, Barlow 2015). These discrepancies may arise from the differential origin of both tissues—circumvallate buds arise from endoderm, whereas fungiform buds presumably arise from ectoderm. Differing developmental mechanisms between anterior and posterior taste fields provides a potential underlying mechanism for the differing phenotypic characteristics found in the present study.

Our observations between anterior and posterior Type III cells largely fit into the separate innervation of these tissues, with one notable exception. The anterior-most foliate papillae is innervated, like the fungiform, by the chorda tympani nerve (a branch of the 7th cranial nerve), whereas the three posterior foliate papillae are innervated by the glossopharyngeal nerve (the 9th cranial nerve). Thus, our study did not divide cells strictly along lines of innervation, providing another potential caveat. If Type III cell characteristics are influenced by nerve identity, our grouping of all foliate papillae as posterior fields may have skewed our results slightly.

Nevertheless, the increased heterogeneity in Type III cells in fungiform and soft palate taste buds suggests that anatomical differences do exist in taste cells, corresponding to the demonstrated functional differences between anterior and posterior taste fields as well as the nerves that innervate them. In both nerve transection experiments and taste cell functional studies, the anterior tongue seems to house relatively specialist taste cells and taste nerve fibers, whereas the posterior tongue is home to more generalist taste cells and nerve fibers (Travers et al. 1987; Frank 1991; Spector and Grill 1992; Hellekant et al. 1997; St. John and Spector 1998; Tomchik et al. 2007; Yoshida et al. 2009). Our data suggest a Type III cell population that, in the posterior taste fields innervated largely by the 9th cranial nerve, is fairly unified by expression markers in comparison to anterior Type III cells innervated by the 7th cranial nerve. This unification in the posterior fields parallels the more generalist nature of cell function there. Increased heterogeneity of expression markers in the anterior tongue, then, suggests that anterior Type III cells are divided into several subcategories. Subgroups of Type III cells could more readily give rise to specialized taste cells, which agrees with the specialized response profiles seen in both fungiform Type III cells and their corresponding nerves.

The specific roles of these putative subgroups of anterior Type III taste cells, however, are unknown. Type III cells have been associated with a variety of functions. PKD2L1-positive cells transduce sour stimuli (Huang et al. 2006; Chang et al. 2010), but Type III cells also play a role in the transduction of salty stimuli as well as carbonation (Chandrashekar et al. 2009; Oka et al. 2013), and possibly water (Zocchi et al. 2017). While amiloride-insensitive salt responses occur in a subset of isolated Type III sour-sensitive cells in the circumvallate taste tissue (Lewandowski et al. 2016), the distribution of response profiles of anterior Type III taste cells is unknown. Perhaps salt-sensitive anterior Type III cells express SNAP25 and accumulate 5-HT but do not express the sour-sensitive marker PKD2L1.

Evidence also exists to suggest that Type III cells play a role in taste signaling between taste cells. Type III cells express purinergic P2Y receptors, which respond to ATP released from Type II cells (Huang et al. 2009). Type II cells in turn respond to both applied 5-HT and GABA, both release products of Type III cells, with a reduction in ATP release (Huang et al. 2009; Dvoryanchikov et al. 2011; Huang et al. 2011). A consequence of this signaling is that the Type III cells that participate in this signaling pathway show small responses to stimuli that are transduced by Type II cells as well as responses to acids and salts (Tomchik et al. 2007). Interestingly, these "broadly tuned" Type III cells are much more abundant in posterior taste fields than anterior fields (Yoshida et al. 2009), bolstering the idea that the Type III cells in anterior fields have more defined functions than in posterior fields.

Our most surprising finding in the current study is a population of GAD67-positive cells that does not express either PKD2L1 or SNAP25. Perhaps, in the anterior tongue, communication between Type II and Type III cells is handled by a subset of Type III cells rather than the whole population. Without SNAP25 to regulate vesicular release, it is perplexing how this cell population would release the GABA it is capable of synthesizing. They would not be the first population in the taste bud to present this puzzle, however. Type I cells express glutamate decarboxylase 65 (GAD65) but do not express the machinery or anatomy associated with vesicle release (Dvoryanchikov et al. 2011).

In the present study, we present an anatomical basis for putative, specialized subgroups of anterior Type III taste cells. The details of specialized function in these Type III cell subcategories in the anterior tongue will require further investigation.

Funding

This work was supported by The National Institutes of Health [R01DC012555 to S.C.K., T32HD041697-13 to C.E.W., F31DC015700 to C.E.W., and R01DC012931 to T.E.F].

Acknowledgements

The authors would like to thank Dr Hiroaki Matsunami for providing the anti-PKD2L1 antibody. We also thank Dr Emily Liman for providing the

PKD2L1-YFP mice used in this study, for helpful discussions about the role of Type III cells in taste buds, and for providing comments on this article.

References

Barlow LA. 2015. Progress and renewal in gustation: new insights into taste bud development. *Development*. 142:3620–3629.

Bo X, Alavi A, Xiang Z, Oglesby I, Ford A, Burnstock G. 1999. Localization of ATP-gated P2X2 and P2X3 receptor immunoreactive nerves in rat taste buds. *Neuroreport*. 10:1107–1111.

Chandrashekar J, Yarmolinsky D, von Buchholtz L, Oka Y, Sly W, Ryba NJ, Zuker CS. 2009. The taste of carbonation. *Science*. 326:443–445.

Chang RB, Waters H, Liman ER. 2010. A proton current drives action potentials in genetically identified sour taste cells. *Proc Natl Acad Sci U S A*. 107:22320–22325.

Chattopadhyaya B, Di Cristo G, Higashiyama H, Knott GW, Kuhlman SJ, Welker E, Huang ZJ. 2004. Experience and activity-dependent maturation of perisomatic GABAergic innervation in primary visual cortex during a postnatal critical period. *J Neurosci*. 24:9598–9611.

Chaudhari N. 2014. Synaptic communication and signal processing among sensory cells in taste buds. *J Physiol*. 592:3387–3392.

Clapp TR, Yang R, Stoick CL, Kinnamon SC, Kinnamon JC. 2004. Morphologic characterization of rat taste receptor cells that express components of the phospholipase C signaling pathway. *J Comp Neurol*. 468:311–321.

DeFazio RA, Dvoryanchikov G, Maruyama Y, Kim JW, Pereira E, Roper SD, Chaudhari N. 2006. Separate populations of receptor cells and presynaptic cells in mouse taste buds. *J Neurosci*. 26:3971–3980.

Dvoryanchikov G, Tomchik SM, Chaudhari N. 2007. Biogenic amine synthesis and uptake in rodent taste buds. *J Comp Neurol*. 505:302–313.

Dvoryanchikov G, Huang YA, Barro-Soria R, Chaudhari N, Roper SD. 2011. GABA, its receptors, and GABAergic inhibition in mouse taste buds. *J Neurosci*. 31:5782–5791.

Frank ME. 1991. Taste-responsive neurons of the glossopharyngeal nerve of the rat. *J Neurophysiol*. 65:1452–1463.

Fujimoto S, Ueda H, Kagawa H. 1987. Immunocytochemistry on the localization of 5-hydroxytryptamine in monkey and rabbit taste buds. *Acta Anat (Basel)*. 128:80–83.

Hellekant G, Danilova V, Ninomiya Y. 1997. Primate sense of taste: behavioral and single chorda tympani and glossopharyngeal nerve fiber recordings in the rhesus monkey, Macaca mulatta. *J Neurophysiol*. 77:978–993.

Huang YA, Dando R, Roper SD. 2009. Autocrine and paracrine roles for ATP and serotonin in mouse taste buds. *J Neurosci*. 29:13909–13918.

Huang YA, Maruyama Y, Roper SD. 2008. Norepinephrine is coreleased with serotonin in mouse taste buds. *J Neurosci*. 28:13088–13093.

Huang YA, Pereira E, Roper SD. 2011. Acid stimulation (sour taste) elicits GABA and serotonin release from mouse taste cells. *PLoS One*. 6:e25471.

Huang YJ, Maruyama Y, Dvoryanchikov G, Pereira E, Chaudhari N, Roper SD. 2007. The role of pannexin 1 hemichannels in ATP release and cell-cell communication in mouse taste buds. *Proc Natl Acad Sci U S A*. 104:6436–6441.

Huang YJ, Maruyama Y, Lu KS, Pereira E, Plonsky I, Baur JE, Wu D, Roper SD. 2005. Mouse taste buds use serotonin as a neurotransmitter. *J Neurosci*. 25:843–847.

Huang AL, Chen X, Hoon MA, Chandrashekar J, Guo W, Tränkner D, Ryba NJ, Zuker CS. 2006. The cells and logic for mammalian sour taste detection. *Nature*. 442:934–938.

Ishimaru Y, Inada H, Kubota M, Zhuang H, Tominaga M, Matsunami H. 2006. Transient receptor potential family members PKD1L3 and PKD2L1 form a candidate sour taste receptor. *Proc Natl Acad Sci U S A*. 103:12569–12574.

Kataoka S, Yang R, Ishimaru Y, Matsunami H, Sévigny J, Kinnamon JC, Finger TE. 2008. The candidate sour taste receptor, PKD2L1, is expressed by type III taste cells in the mouse. *Chem Senses*. 33:243–254.

Kim DJ, Roper SD. 1995. Localization of serotonin in taste buds: a comparative study in four vertebrates. *J Comp Neurol*. 353:364–370.

Lewandowski BC, Sukumaran SK, Margolskee RF, Bachmanov AA. 2016. Amiloride-insensitive salt taste is mediated by two populations of Type III taste cells with distinct transduction mechanisms. *J Neurosci*. 36:1942–1953.

Ma H, Yang R, Thomas SM, Kinnamon JC. 2007. Qualitative and quantitative differences between taste buds of the rat and mouse. *BMC Neurosci*. 8:5.

Murray RG. 1993. Cellular relations in mouse circumvallate taste buds. *Microsc Res Tech*. 26:209–224.

Murray RG, Murray A. 1971. Relations and possible significance of taste bud cells. *Contrib Sens Physiol*. 5:47–95.

Nada O, Hirata K. 1975. The occurrence of the cell type containing a specific monoamine in the taste bud of the rabbit's foliate papila. *Histochemistry*. 43:237–240.

Ohtubo Y, Yoshii K. 2011. Quantitative analysis of taste bud cell numbers in fungiform and soft palate taste buds of mice. *Brain Res*. 1367:13–21.

Oka Y, Butnaru M, von Buchholtz L, Ryba NJ, Zuker CS. 2013. High salt recruits aversive taste pathways. *Nature*. 494:472–475.

Perea-Martinez I, Nagai T, Chaudhari N. 2013. Functional cell types in taste buds have distinct longevities. *PLoS One*. 8:e53399.

Pumplin DW, Yu C, Smith DV. 1997. Light and dark cells of rat vallate taste buds are morphologically distinct cell types. *J Comp Neurol*. 378:389–410.

Roberts CD, Dvoryanchikov G, Roper SD, Chaudhari N. 2009. Interaction between the second messengers cAMP and Ca2+ in mouse presynaptic taste cells. *J Physiol*. 587:1657–1668.

Roper SD. 2013. Taste buds as peripheral chemosensory processors. *Semin Cell Dev Biol*. 24:71–79.

Royer SM, Kinnamon JC. 1988. Ultrastructure of mouse foliate taste buds: synaptic and nonsynaptic interactions between taste cells and nerve fibers. *J Comp Neurol*. 270:11–24, 58–9.

Royer SM, Kinnamon JC. 1991. HVEM serial-section analysis of rabbit foliate taste buds: I. Type III cells and their synapses. *J Comp Neurol*. 306:49–72.

Spector AC, Grill HJ. 1992. Salt taste discrimination after bilateral section of the chorda tympani or glossopharyngeal nerves. *Am J Physiol*. 263:R169–R176.

St John SJ, Spector AC. 1998. Behavioral discrimination between quinine and KCl is dependent on input from the seventh cranial nerve: implications for the functional roles of the gustatory nerves in rats. *J Neurosci*. 18:4353–4362.

Taruno A, Vingtdeux V, Ohmoto M, Ma Z, Dvoryanchikov G, Li A, Adrien L, Zhao H, Leung S, Abernethy M, *et al.* 2013. CALHM1 ion channel mediates purinergic neurotransmission of sweet, bitter and umami tastes. *Nature*. 495:223–226.

Tomchik SM, Berg S, Kim JW, Chaudhari N, Roper SD. 2007. Breadth of tuning and taste coding in mammalian taste buds. *J Neurosci*. 27:10840–10848.

Travers JB, Grill HJ, Norgren R. 1987. The effects of glossopharyngeal and chorda tympani nerve cuts on the ingestion and rejection of sapid stimuli: an electromyographic analysis in the rat. *Behav Brain Res*. 25:233–246.

Vandenbeuch A, Zorec R, Kinnamon SC. 2010. Capacitance measurements of regulated exocytosis in mouse taste cells. *J Neurosci*. 30:14695–14701.

Yang R, Crowley HH, Rock ME, Kinnamon JC. 2000. Taste cells with synapses in rat circumvallate papillae display SNAP-25-like immunoreactivity. *J Comp Neurol*. 424:205–215.

Ye W, Chang RB, Bushman JD, Tu YH, Mulhall EM, Wilson CE, Cooper AJ, Chick WS, Hill-Eubanks DC, Nelson MT, *et al.* 2016. The K+ channel KIR2.1 functions in tandem with proton influx to mediate sour taste transduction. *Proc Natl Acad Sci U S A*. 113:E229–E238.

Yee CL, Yang R, Böttger B, Finger TE, Kinnamon JC. 2001. "Type III" cells of rat taste buds: immunohistochemical and ultrastructural studies of neuron-specific enolase, protein gene product 9.5, and serotonin. *J Comp Neurol*. 440:97–108.

Yoshida R, Miyauchi A, Yasuo T, Jyotaki M, Murata Y, Yasumatsu K, Shigemura N, Yanagawa Y, Obata K, Ueno H, *et al.* 2009. Discrimination of taste qualities among mouse fungiform taste bud cells. *J Physiol*. 587:4425–4439.

Zocchi D, Wennemuth G, Oka Y. 2017. The cellular mechanism for water detection in the mammalian taste system. *Nat Neurosci*. doi:10.1038/nn.4575